COMMISSIONING OF A DIODE / RF PHOTOGUN COMBINATION

R. Ganter, B. Beutner, S. Binder, H.H. Braun, M. Broennimann, M. Dach, T. Garvey, C. Gough, C. Hauri, M. Heiniger, R. Ischebeck, S. Ivkovic, Y. Kim, E. Kirk, F. Le Pimpec, K. Li, R. Luescher, P. Ming, A. Oppelt, M.L. Paraliev, M. Pedrozzi, J.-Y. Raguin, T. Schietinger, T. Schilcher, B. Steffen, L. Rivkin, S. Tsujino, A. Wrulich, Paul Scherrer Institut, 5232 Villigen PSI, Switzerland

Abstract

Tests of an electron gun based on diode acceleration followed by a two-cell RF cavity at 1.5 GHz are being performed at PSI. The diode consists of a photocathode / anode assembly and is driven by a voltage pulse of 500 kV maximum in 200 ns FWHM. The diode configuration allows various types of cathode geometries including hollow cathode with field emitter array (FEA) inserts. In addition the diode assembly gives full control of the position, direction and size of the electron beam at the RF cavity entrance plane. Comparisons between simulations and measurements are presented for the case of a simplified elliptical photocathode geometry. First tests with a specially designed hollow cathode reveal a beam emittance below 0.5 mm.mrad for 10 pC charge.

INTRODUCTION

In the context of the SwissFEL project [1] [2], studies of electron gun concepts providing low emittance beams started a few years ago at PSI [3] [4]. The gun presented here is a combination of diode acceleration followed by a two-cell RF cavity at 1.5 GHz. Such a configuration was first motivated by the possibility of inserting field emitter arrays [5] within the cathode. In the meantime it became clear that the use of the cathode as a simple photocathode together with the different pulser features (cathode motorization in six directions, high surface gradient, pulsed solenoid, electrostatic focusing with diode geometry) offers new possibilities to control the trajectory and shape of the electron beam before it enters the RF cavity for further acceleration.

DIODE / RF GUN DESCRIPTION

The diode is a cathode - anode assembly (see Fig. 1) separated by a gap, g ($0 < g < 30$ mm), across which voltage pulses are applied with 200 ns FWHM duration and maximum amplitude of V_{Pulser} = 500 kV [6]. Electrons are extracted from the cathode by photoemission using laser pulses at 262 nm wavelength from a Nd:YLF regenerative laser [7].

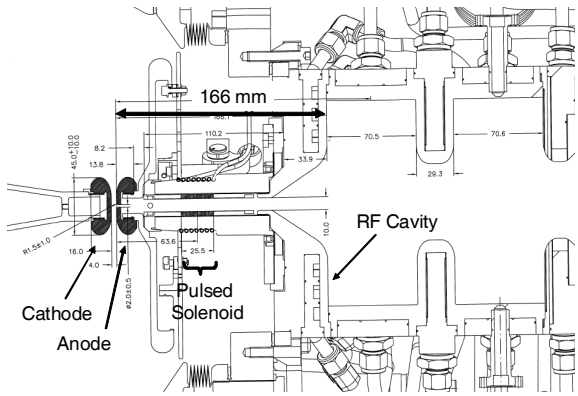

Figure 1: Section through the diode / RF gun combination. (Here the cathode and anode have a flat geometry)

The laser has transversally a flat top profile with diameter D_{laser} ($0.5 < D_{laser} < 1.8$ mm) but it has a Gaussian longitudinal shape with a duration, $\sigma_{t,laser}$ = 4.2 ps (rms). Seen by the beam, the pulsed diode (200 ns FWHM) is like a DC acceleration. For mechanical reasons, the anode is separated from the RF cavity entrance plane by a drift distance of $d_{anode\text{-}RF}$ = 166 mm. To prevent an expansion of the beam during the drift and to match the beam to the RF acceleration [8], a 25 mm long pulsed solenoid is located 51 mm after the anode iris. The pulsed solenoid consists of a coil concentric with a ring, the inner ring has a diameter of 1 cm [9]. Current pulses of up to 2 kA and 100 µs duration are sent to the outer coil, leading to a maximum magnetic field of B_{PSL} = 320 mT on axis [10,11]. This pulsed solenoid technology was chosen in order to fit the available space between the diode and the RF cavity. In addition the solenoid fields towards the cathode are then naturally shielded by the eddy currents in the surrounding materials. The two-cell RF cavity has a frequency of 1.5 GHz [11] and is fed with an RF forward power P_{RF} of 4 to 5 MW with 5 µs pulses, corresponding to an accelerating gradient between 40 and 45 MV/m. The repetition rate of laser, pulser and RF is

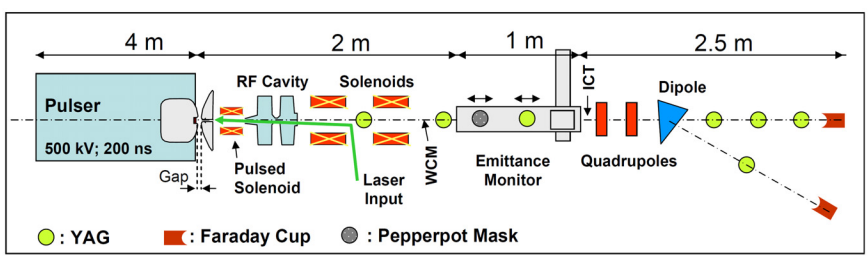

Figure 2: Schematic of the Diode – RF gun and diagnostic beam line.

presently limited to 10 Hz. Figure 2 shows a schematic of the full diagnostic beamline which follows the electron gun. Seven YAG screens along the beam axis allow measurements of the transverse beam profile. The two solenoid magnets following the RF cavity focus the beam in the emittance monitor. They can provide a maximum field of B_{DSL}= 250 mT and are 0.2 m long. Eight pairs of vertical and horizontal corrector magnets (0.5 mT maximum field; 1 cm length) are distributed along the axis downstream of the RF cavity. Projected emittances are measured with a pepper-pot technique at different locations along the emittance monitor [12] (Fig. 3). A spectrometer setup made of one dipole and two equally spaced screens follows the emittance monitor [13]. The dispersive arm makes a 30 degree angle with the gun axis and the dipole is 230 mm long. The nominal field required for a 4 MeV beam, B_{dipole} = 34 mT. A quadrupole doublet in front of the dipole provides a sharp horizontal focus and limits the beam size vertically on the spectrometer arm screen. Various beam charge diagnostics (wall current monitor (WCM), integrating current transformer (ICT) and Faraday cups) are distributed along the machine (Fig. 2).

DIODE / RF GUN COMMISSIONING

Target Gun Parameters

The targeted parameters with this diode and RF cavity combination are a normalized projected rms emittance below 0.5 mm.mrad with a charge, Q = 200 pC, a peak current, I_{peak}= 22 A and a kinetic energy, E = 5 MeV. ASTRA [14] simulations show that this is possible with a standard photocathode only if electrostatic focusing is applied in the diode part of the gun [15]. This can be obtained with the hollow cathode geometry presented in figure 7, where the lips surrounding the cathode insert focus the electric field lines. During the commissioning of the gun, a simplified cathode geometry was used (elliptical shape). The elliptical shape is easier to manufacture and polish in case of replacement after breakdown in the diode. Tests of the maximum achievable electric gradient were performed in parallel to the machine commissioning. With "Diamond Like Carbon" (DLC) coating on both cathode and anode a gradient as high as 100 MV/m (V_{Pulser} = 300 kV; gap = 3 mm) could be sustained during weeks without breakdown. Breakdown limit on 16 electrode pairs has been measured to be between 150 MV/m and 320 MV/m. This coating was then also applied to the hollow cathode geometry. Although the elliptical cathode produces a larger emittance than the target value, it enables us to gain experience tuning the machine and to make comparison with simulations as shown in Figs. 5 and 6.

Momentum Measurements

Figure 3 shows the typical beam shape produced by the diode / RF gun with the elliptical cathode. The shape is not perfectly round in this example probably because of some slight misalignment. The bottom part of the figure shows the corresponding pepper-pot image obtained in the emittance monitor. From the image, the rms normalized projected emittance can be determined, in this case $\varepsilon_{n,x}$=1.2 ± 0.2 mm.mrad. All emittances presented in this paper were measured with the pepper-pot method [16].

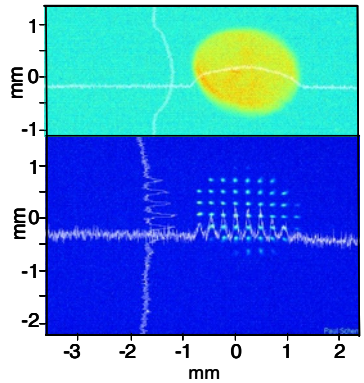

Figure 3: Electron beam on a YAG screen in the emittance monitor (top) and when a pepper-pot mask is inserted 50 mm upstream (bottom) (E = 4.4 MeV; Q = 12 pC; D_{laser}= 0.5 mm; V_{Pulser} = 300 kV; gap = 6 mm; B_{PSL} = 130 mT; B_{DSL1}= 100 mT; B_{DSL2}= 89 mT)

The spectrometer arm enables the measurement of the mean momentum and momentum spread as a function of the RF phase (see Fig. 4). The minimum uncorrelated energy spread is 4 keV (rms) for a laser pulse duration of 4.2 ps rms. The typical stability of the RF phase is around 1 degree (peak to peak) leading to energy fluctuations between bunches of 20 keV (peak to peak).

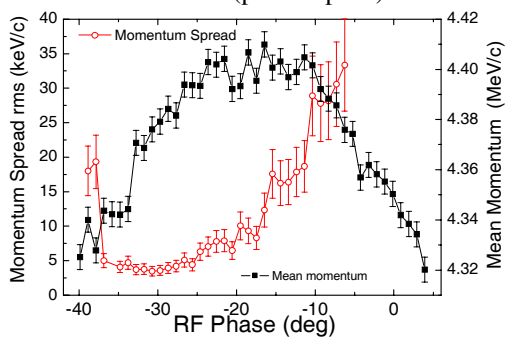

Figure 4: Momentum and momentum spread versus the RF Phase φ_{RF} (E = 4.4 MeV; B_{dipole}= 36 mT; Q = 18 pC; D_{laser}= 0.5 mm; V_{Pulser} = 300 kV; Gap = 6 mm; P_{RF}= 4.35 MW; B_{PSL} = 130 mT; B_{DSL1}= 71 mT; B_{DSL2}= 60 mT)

Comparison Simulations / Measurements

Simulations of the beam dynamics in the case of elliptical electrodes were performed with the code OPAL [17] and compared to measurements. Figure 5 shows a comparison between the measured and calculated beam size along the machine axis. The first measurement screen is at z ~ 1.2 m, just after the in-coupling laser mirror. Several measurements with the same machine parameters, but acquired on different days, are shown and give an idea of the beam reproducibility. The agreement with simulation is relatively good, given that simulations assume an ideal flat top profile for the transverse laser

intensity distribution. In reality, variations as large as 20 % [7] are present in the laser transverse intensity distribution.

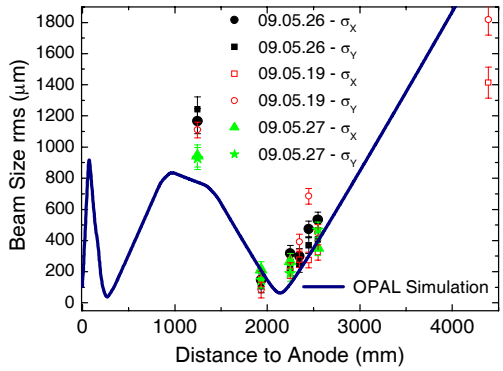

Figure 5: Transverse electron beam size (rms) along the machine axis simulated and measured on different days. (E = 4.4 MeV; Q = 10 pC; D_{laser}= 0.9 mm; V_{Pulser} = 300 kV; Gap = 6 mm; φ_{RF} = -25 deg; B_{PSL} = 130 mT; B_{DSL1}= 116 mT; B_{DSL2}= 87 mT)

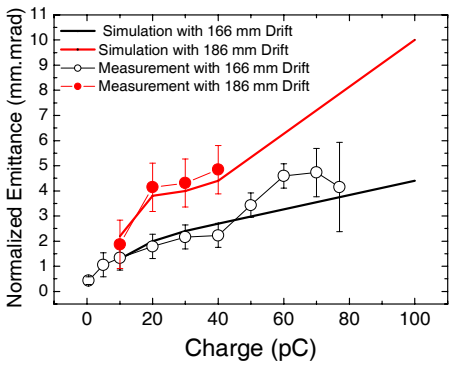

Figure 6: Normalized rms projected emittance versus the bunch charge for two different distances $d_{Anode\text{-}RF}$. (E = 4.4 MeV; D_{laser}= 1.4 mm; V_{Pulser} = 300 kV; Gap = 6 mm)

Reasonable agreement was obtained between measured and simulated (OPAL) emittance values as shown in Figure 6. The machine parameters have been optimized for the highest charge and were kept constant while decreasing the charge (attenuation of laser intensity). Pepper-pot images were analysed with the XanaROOT application [18]. After subtraction of a background image, the full image projection is fitted with a sum of Gaussians to determine beamlet widths. All presented emittances were obtained by only considering the central 90 % of the horizontal or vertical beam projections. The error bars come mainly from the beamlet width estimations and background noise. Figure 6 clearly shows that with the elliptical electrodes the emittance values grow rapidly up to 4 mm.mrad (in the case of $d_{Anode\text{-}RF}$ =166 mm). In fact, during the drift from the anode to RF cavity (more exactly between the anode and the pulsed solenoid), space charge effects increase the emittance to a level where no compensation applies anymore. For the same reason the emittance is more than doubled when $d_{Anode\text{-}RF}$ is increased from 166 mm to 186 mm, at high charge (see Fig. 6). One way to limit this emittance growth is to apply transverse focusing by shaping the cathode geometry (see Figure 7). As for a Pierce-type geometry, the transverse electrostatic focusing can be used to compensate the space charge effects in the gap and the beam enters the remaining drift better focussed [16].

Electrostatic Focusing with Hollow Cathode

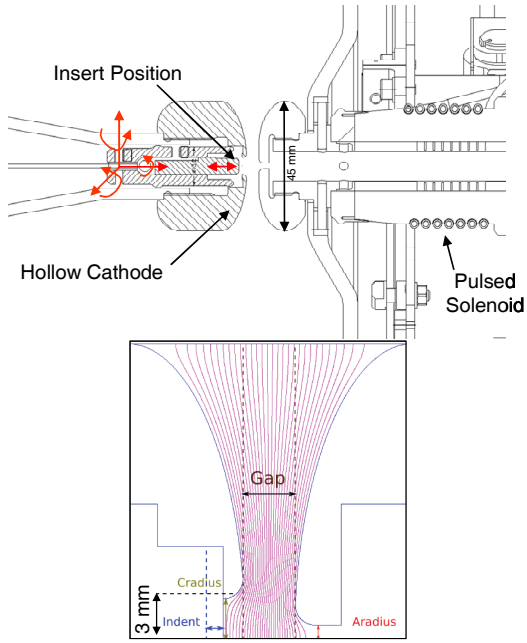

Figure 7: Top: Cut view of the diode assembly with the hollow cathode geometry. Bottom: Zoom on the hollow cathode geometry showing the potential lines.

As stated above, electrostatic focusing in the diode part can partially compensate the emittance growth due to space charge in the drift space between anode and RF cavity. Figure 7 (bottom) presents a POISSON simulation [19] of the so-called hollow cathode geometry. This design allows one to place an insert (FEA or different photo-cathode material) at the centre of the cathode. The two lips holding the cathode insert deform the equipotential lines and provide a transverse focusing to the electron beam. The hollow cathode has been coated with DLC as mentioned earlier. In the following, the chosen gradient on the surface of the hollow cathode was 80 MV/m leading to a gradient of ~ 40 MV/m in the middle of the insert surface. The top part of Figure 7 shows the full diode assembly with the hollow cathode. There is a possibility to adjust the insert position depth to optimise the electrostatic focusing.

ASTRA [14] simulations with this geometry were performed and predicted an emittance of 0.5 mm.mrad with Q= 200 pC when using a longitudinally flat top laser profile (10 ps long, 0.7 ps rise and fall times) [15]. A Ti:sapphire laser system is currently under preparation at PSI to provide such laser pulses in the near future [7]. Nevertheless, the Gaussian longitudinal laser pulses provided by the currently installed Nd:YLF laser can still be used to compare the emittance reduction when

changing from an elliptical cathode to the hollow cathode geometry.

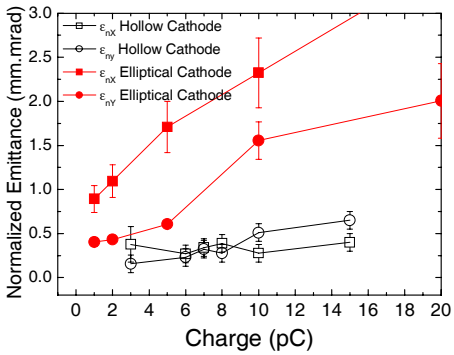

Figure 8: Normalized rms projected emittance versus the bunch charge for the two cathode geometry (E = 4.4 MeV; D_{laser}= 1.4 mm; V_{Pulser} = 300 kV; $Gap_{ellipt.}$ = 6 mm / $Gap_{hollow.}$ = 4 mm)

First measurements of the emittance with the hollow cathode geometry were performed and results are shown in Figure 8. The insert used within the hollow cathode was a 7x7 mm Mo chip on which one FEA pyramid (see Fig. 9) has been deposited [5]. It is not clear how far this unique pyramid (3 µm in size) centred in the insert influenced the photoelectron beam current density distribution. The laser beam illuminated an area of 1.4 mm diameter and electrons were probably emitted from the whole illuminated area of the chip. With an applied gradient of 40 MV/m on the insert no field emitted charges have been detected but local field enhancement could have had an effect on the quantum efficiency distribution.

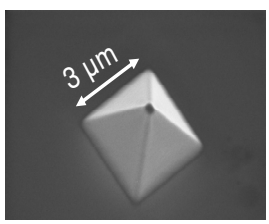

Figure 9: SEM picture of the Mo pyramid in the middle of the chip-insert held by the hollow cathode.

In any case, figure 8 clearly shows a reduction of the emittance when going from the elliptical cathode geometry to the hollow cathode geometry with the single tip insert. Emittances as low as 0.2 mm.mrad were obtained with 6 pC charge and a Gaussian laser pulse of 4.2 ps duration (rms). Measurements with higher charge are not yet possible due to limitations in the available laser energy. However, this result is encouraging for future tests when the Ti:sapphire laser with higher intensity and longitudinal pulse shaping will be brought into operation.

SUMMARY

The commissioning of an accelerating diode / RF gun assembly has been initiated at PSI. The key elements of the machine (magnets, pulser, laser, RF power plant and diagnostics) are operational and electron beam with energy up to 5 MeV can routinely be produced and diagnosed. Particular care was taken with the emittance diagnostic (quality of pepper-pot images and analysis tool (XanaROOT)). Stable operation with surface electric fields of 100 MV/m for periods of several weeks could be demonstrated with the DLC coating on both electrodes. The chosen hollow cathode geometry gives encouraging emittance values as low as 0.2 mm.mrad with 6 pC. The hollow cathode held a chip with one deposited pyramid tip. Although the influence of this pyramid tip on the beam quality is not clear it opens the possibility of inserting other kind of field emitters such as needle cathodes [20] and field emitter arrays with built-in gate electrodes [21]. Before testing special field emitter cathode inserts, the next step will be to produce the target parameters predicted by simulation (0.5 mm.mrad at 200 pC) with a flat insert and flat-top laser profile (10 ps).

REFERENCES

[1] http://fel.web.psi.ch
[2] B. D. Patterson, (Editor) PSI-SwissFEL Science Case (to be published).
[3] R. Ganter *et al.*, Proceedings of the FEL Conference, Trieste - Italy, 2004, p. 602-605.
[4] R. Ganter *et al.*, Proceedings of the EPAC Conference, Lucerne - Switzerland, 2004, p. 306-308.
[5] E. Kirk *et al.*, J. Vac. Sci. Technol. B **27,** 1813-1820 (2009).
[6] M. Paraliev, C. Gough, and S. Ivkovic, Proceedings of the IEEE Power Modulator Conference Conference, Las Vegas, USA, 2008.
[7] C. Hauri, R. Ganter, and P. F. Ple, Proceedings of the this conference, 2009.
[8] C.-X. Wang *et al.*, Phys. Rev. ST Accel. Beams **10,** 104201 (2007).
[9] M. Paraliev, PSI Report No. FEL-PA84-005-0 (2008).
[10] M. Paraliev, C. Gough, and S. Ivkovic,(to be published).
[11] K. Li, Thesis, ETH Zurich (No. 18168), 2008.
[12] V. Schlott *et al.*, Proceedings of the Diagnostic Particle Accelerator Conference (DIPAC2007) Conference, Ve nice (Italy), 2007.
[13] A. Streun, PSIReport No. FEL-SA84-001-1 (2007).
[14] http://www.desy.de/~mpyflo/
[15] K. Li, PSI Report No. FEL-LK06-004-01 (2009).
[16] M. Reiser, *Theory and Design of Charged Particle Beams, pp. 564-566* (John Wiley & Sons, New-York, 1994).
[17] A. Adelmann *et al.*, Proceedings of the PAC2009 Conference, Vancouver (Canada), 2009.
[18] amas.web.psi.ch/tools/XanaROOT/.
[19] http://laacg.lanl.gov/laacg/services/
[20] R. Ganter *et al.*, Phys. Rev. Letters **100,** 064801 (2008).
[21] S. Tsujino *et al.*, Appl. Phys. Letters **92,** 193501 (2008).